Theoretical Determination of the NMR Spectrum of Liquid Ethanol

Piotr Zarzycki*,†,‡ and James R. Rustad†

Department of Geology, University of California, One Shields Avenue, Davis, California 95661, and Environmental Molecular Sciences Laboratory, Pacific Northwest National Laboratory, P.O. Box 999, K8-96, Richland, Washington 99352

Received: June 30, 2008; Revised Manuscript Received: November 14, 2008

Gauge-invariant NMR chemical shifts of the C and H sites in ethanol is calculated over a variety of conformational and solvation environments using density functional methods. The effects of different exchange and correlation functionals and different basis sets are systematically explored. While there is often a good correlation between atomic charges, as calculated using population analysis techniques, and calculated chemical shifts, we show that calculated populations can only be used as a rough guide to estimating the magnitude of the chemical shift. To incorporate solvent, we use configurations sampled from a classical molecular dynamics simulation of solvated ethanol. We show that the calculated NMR chemical shift at the alcohol proton converges to the experimental result provided that a sufficient number of solvent molecules are included in the GIAO calculation. The predicted shift is in much better agreement with experiment than the shift predicted from clusters with fully optimized solvation shells because of the tendency of solvents to overbond to the alcohol proton in fully optimized configurations.

1. Introduction

The magnetic fields at nuclear sites (e.g., ^{1}H and ^{13}C) within molecules are modified by circulating charge in the surrounding electron cloud. Consequently, the magnetic field at a given nucleus differs from the externally applied magnetic field. The density and magnetic response of the cloud varies with chemical environment. The difference between the applied field and the total field at the nucleus can be expressed through a magnetic shielding constant, called the chemical shift σ, which is the basis of NMR spectroscopy. The chemical shift is a function of the magnetic field intensity, and is defined as the difference between the magnetic shielding constants (σ) for a given molecule and a reference compound ($\delta = \sigma^{ref} - \sigma$), most commonly tetramethylsilane (TMS).

If the chemical shift (δ) for a given nucleus is higher than zero, the nucleus is said to be more deshielded, and if δ is less than zero the nucleus is more shielded than the corresponding nucleus in the reference (TMS). The magnetic field at a deshielded nucleus is closer to the applied field than it would be in the reference compound. The extent of deshielding of a proton nucleus can be estimated by considering the electronegativities of the nearby atoms. The higher these electronegativities, the lower electron density around the proton and, consequently, the more positive the chemical shift is. The tendency for nuclei to pair their spins with one of the bonding electrons causes coupling between nuclei sharing a chemical bond. In general coupling is important on the range of two (geminal coupling, ^2J) and three (vicinal coupling, ^3J) bonds. Moreover, spin-coupling is stronger for ^{1}H NMR than ^{13}C NMR.[1] Spin coupling causes the presence of multiplets on NMR spectra.

The structure and properties of protonic liquids like water and ethanol are determined to a large extent by the arrangements of hydrogen bonds. Hydrogen bonding into the oxygen in an OH group stabilizes negative charge on the oxide ion and therefore decreases the electron density on a hydroxylic proton. The nucleus of the hydroxylic proton is more exposed than H in TMS and has a positive δ. The hydroxylic ^{1}H NMR peak in alcohols is usually located between 0.5−4.0 ppm. Its actual position depends on concentration, temperature, and other factors affecting the hydrogen-bond network in the system.[1]

The NMR spectrum of ethanol has been experimentally well explored. There are three kinds of chemically different protons in the ethanol molecule. At ambient temperature, thermal rotation about the C−C bond causes all protons in the CH_3 and the CH_2 groups to become equivalent on the NMR time scale. In the ^{1}H NMR spectrum of liquid ethanol we observe three peaks in the following order $\delta_{OH} > \delta_{CH_2} > \delta_{CH_3}$. The peak for methyl protons is usually a triplet (vicinal coupling to the methylene group), and the peak for methylene protons is a quartet (vicinal coupling to the methyl group). Vicinal coupling of the OH proton to methylene protons should result in a triplet peak, however when the system is exposed to water vapor (air) rapid proton exchange causes the coupling to disappear (OH proton peak becomes a singlet).[1]

In the gas phase the OH proton has a lower diamagetic shielding than the CH_2 and CH_3 protons and the sequence is as follows: $\delta_{CH_2} > \delta_{CH_3} > \delta_{OH}$. This sequence has been reproduced in gas-phase electronic structure calculations of the chemical shift.[3]

The position of OH proton peak for ethanol dissolved in liquids depends on hydrogen bonding environment. For example, the hydroxylic proton of ethanol dissolved in $CDCl_3$ (dielectric constant $\sim$ 5 is located between CH_3 and CH_2 at $\delta \sim 2.57$ ppm whereas in the DMSO-d_6 (dielectric constant $\sim$ 47) it has the highest chemical shift in spectrum at $\delta \sim 4.32$ ppm.[1]

Steric effects in liquids also affect the conformational variability of ethanol. In the ^{1}H NMR spectrum of CH_3/CH_2

* Correspondence address: Environmental Molecular Sciences Laboratory, Pacific Northwest National Laboratory. Fax: 509-3716354. E-mail: piotr.zarzycki@pnl.gov.
† Department of Geology, University of California.
‡ Environmental Molecular Sciences Laboratory, Pacific Northwest National Laboratory.

10.1021/jp805737a CCC: $40.75
Published on Web 12/12/2008

group, rapid rotation about the carbon−carbon bond causes the chemical shift to become equivalent, however, modern high-frequency NMR spectrometers are able to distinguish different rotational isomers.[4,5] The rotation dynamics of isotope-substituted peptides can be easily detected by the NMR-spectrometer, however, for small molecules (like C_2H_5OH) the NMR-spectrum is usually averaged over many conformations. According to Karplus,[6] the extent of vicinal coupling between the hydroxylic and methylene protons is correlated with the dihedral angle (H−C−C−H or H−C−O−H). Since the conformations of molecules in liquids are mostly determined by inter- and intramolecular interactions, we cannot expect to observe only energetically stable configurations, especially if the hydrogen-bonding energy is comparable with energetic barrier for rotation.

In this paper, we examine the effect of conformation and solvation on the NMR spectrum of ethanol. We present extensive calculations in the gas phase looking at the influence of conformational variability on the chemical shifts of the constituent atoms (Supporting Information). In addition, we present the results of a series of population analysis methods and assess the degree to which they correlate with the calculated chemical shifts (Supporting Information). We perform a molecular dynamics simulation of liquid ethanol and periodically extract first-shell solvent configurations about particular ethanol molecules. These configurations are then used in an electronic structure code to calculate NMR chemical shifts. These configurations explore the conformational space of the ethanol molecule in the solvent as well as the dynamic rearrangement of neighboring ethanol molecules in the solvation sphere of the central ethanol molecule. Because the NMR spectrum is influenced by both solvation and conformational effects, the calculations can help to unravel the different contributions. The solvent molecules are included explicitly so all special effects (especially the hydrogen-bonds) can be easily studied.

2. Theory

The theoretical prediction of magnetic shielding constants is based on perturbation theory, where the external and internal magnetic field are treated as a perturbation. Due to the environment about the nucleus, defined by the presence of other nuclei and electrons, the local magnetic field differs from the external magnetic field, so, the perturbation is a function of nuclear positions and electron density.

As a result of the perturbation analysis one obtains the magnetic shielding $\bar{\sigma}$ (second-order asymmetric tensor) and the magnetic susceptibilities $\bar{\chi}$ (second-order symmetric tensor).[7−9] The magnetic shielding tensor for a given nucleus k is composed of the elements:

$$\sigma^k_{\alpha\beta} = \left(\frac{\partial^2 E}{\partial \mu^k_\alpha \, \partial B_\beta}\right) \quad \text{where } \alpha, \beta = x, y, z \tag{1}$$

where $\vec{\mu}$ is the magnetic moment of a nucleus. The magnetic shielding constant is difficult to compute because for any incomplete basis set, the calculated magnetic properties depend on the gauge origin.[7−9] This is called the gauge-origin problem. Thus, in the theoretical prediction of NMR spectra, we are faced with the choice of electronic structure calculation scheme and the algorithm used to predict gauge-invariant magnetic shielding constants. At present, there are a few schemes designed to calculate gauge-invariant chemical shifts: IGLO (individual gauge for localized orbitals),[10] GIAO (gauge including atomic orbitals),[7,11−13] LORG (localized orbital local origin),[14] CSGT (continuous set of gauge transformations)[15] and IGAIM (individual gauges for atoms in molecules).[15] Due to the fact that GIAO converges faster than the IGLO and LORG methods, it is usually used for expensive calculations. Unlike GIAO, IGLO and LORG can also yield magnetic susceptibilities.[9]

For the sake of consistency, the magnetic shielding constant for the reference (in our case TMS) is calculated on the same level of theory as for the ethanol conformer.

To some extent the local nucleus shielding is determined by the local electron density and its flux during molecular motion.

2.1. Charge Flow and Asymmetry. For NMR calculations, the electron density around a given nucleus, in a given nuclear basis (in the sense of Bader's theory of atoms in molecule[16]) is of central importance. The dipole moment is a measure of the asymmetry in charge distribution along the whole molecule. The flow of charge between the nuclei during rotation or bond stretching and the dynamics of charge distribution can be studied in more detail in terms of atomic charge concepts. Unfortunately, atomic charge is not a direct quantum observation, and can be only predicted by using some partitioning schemes for analyzing electronic populations. There are three general classes of population analysis:[17] partitioning of Hilbert space (e.g., Mulliken, Löwdin, Weinhold), partitioning of real space (Bader, Hirschfield) and fitting the charges to reproduce the electrostatic potential (e.g., Merz−Singh−Kollman).

Even if the dipole moment is a good estimator of charge asymmetry in the molecule, it does not describe local charge asymmetry and subtle charge flow observed for the conformational motion.[19] It can be used, however, as a particularly simple standpoint from which to analyze conformational effects on the chemical shift.

2.2. Simulation Details. To supply conformations for the chemical shift calculations, we performed the classical Molecular Dynamics simulations of liquid ethanol at constant temperature (T = 298 K) and volume (d = 0.787 g/cm^3) using the Verlet integration scheme and the Nóse-Hoover thermostat.[20,21] The computational cell contains 100 ethanol molecules periodically replicated in each direction. The interactions are described by the OPLS/AA force field (optimized potential for liquid simulations/all atoms) proposed by Jorgensen.[22,23] The Lennard-Jones interactions were calculated using a spherical cutoff (r_c = 9 Å) and the long-range electrostatic interactions (from the OPLS/AA partial charge) were calculated using the Ewald summation. The constraints within ethanol molecules were enforced using the SHAKE algorithm. Molecular dynamics simulations were carried for 250 ps (2.5×10^5 steps, time interval Δt = 0.001 ps). The configurations were stored after 100 ps of simulation run (equilibration). The configurations were generated at 50-step intervals (after equilibration), which means that successive snapshots are separated by 0.05 ps.

We also calculate radial distribution functions (to define cluster extraction criteria) and the self-diffusion coefficients (to assess conformational sampling and check the calculations). Hydrogen-bond analysis is based on the following criteria for existence of hydrogen bond: $|\angle OOH| \leq 30^o$ and $r_{OO} \leq$ 3.5 Å.

Initially, our intention was to calculate the magnetic shielding constants for each molecule in each snapshot. However, the calculations for 900 atoms (100 molecules in each time frame snapshot) with 6-311++G(d,p) basis set was too expensive for 1000 configurations. We decided to extract some subset of

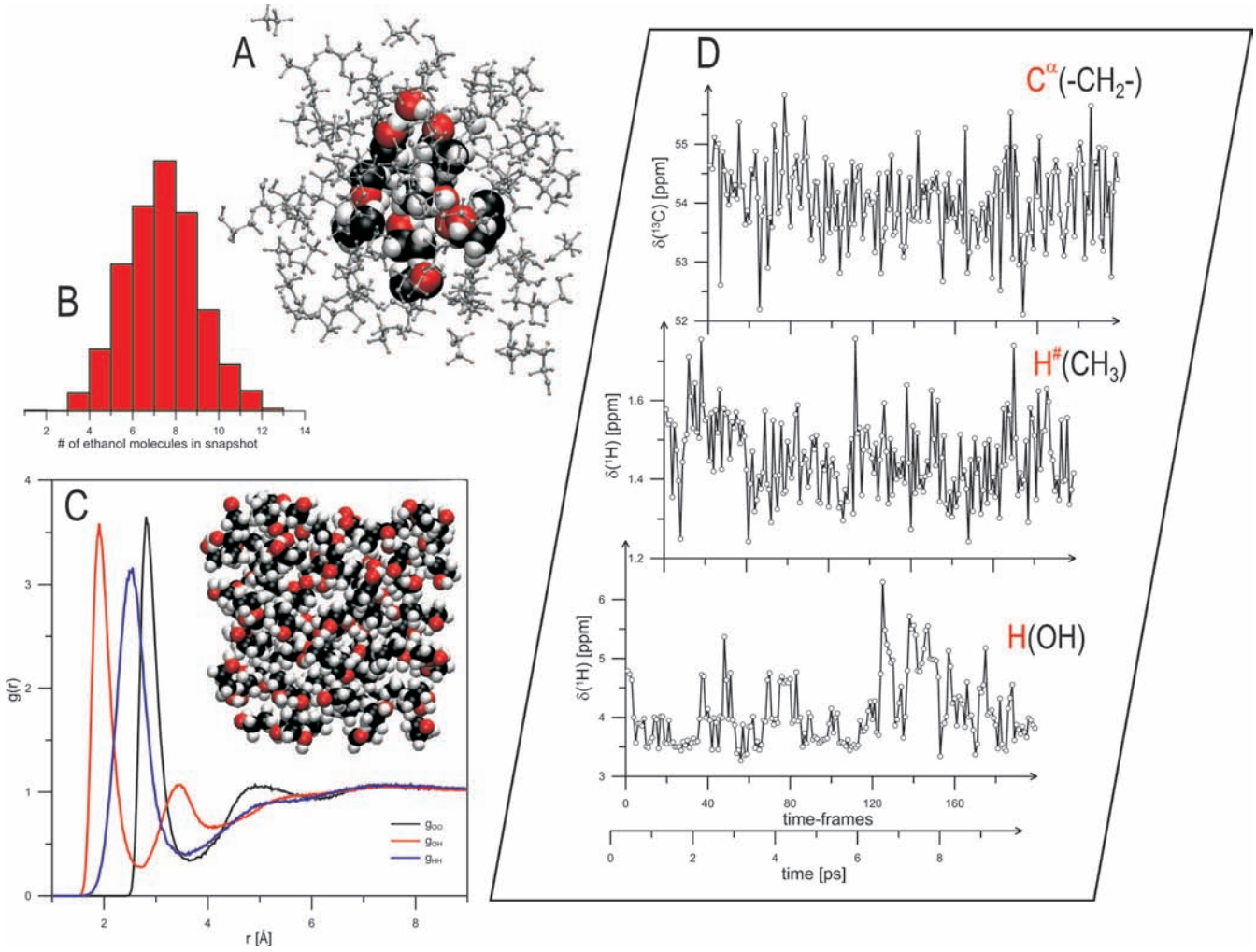

Figure 1. Quantum calculation along classical trajectory. In part A, the subsystem subjected to quantum measurement is shown. In part B, the probability distribution for number of molecules in subsystem (number of ethanol molecules in sphere $r_{OO} = 6$ Å). In part C, the radial distribution functions for (oxygen−oxygen, hydroxyl proton−hydroxyl proton, oxygen−hydroxyl proton) ethanol liquid are shown. In part D, the examples of chemical shifts time dependence (subsystem averaged) for 10 ps observation window are shown.

trajectory by choosing a reference molecule extracting it with the spherical environment of other molecules (at cutoff $r_{OO} =$ 6 Å).

The time-averaged chemical shift can be calculated as

$$\langle \delta_k \rangle_{time(N_p,N_t,N_a)} = \frac{1}{N_p}\sum_{i}^{N_p}\frac{1}{N_t}\sum_{j}^{N_t}\frac{1}{N_a}\sum_{l}^{N_a}\delta_{k(i,j,l)} \equiv \langle\langle\langle \delta_k \rangle_{N_a}\rangle_{N_t}\rangle_{N_p} \tag{2}$$

where N_p stands for number of trajectories (track of different ethanol molecule and their environment), N_t is the number of analyzed time-frames, and N_a is number of k-atoms in a given j-frame. Due to the simplicity of our system, we trace only one ethanol molecule within its neighbors, so in our case $N_p = 1$.

There are two cases which arise immediately: time-origin invariance and space-time correlation between the subsequent MD configurations. First of all, there is no distinctive time-configuration, so we can start to collect system snapshots at any time after equilibration is established. We can also observe the system for a given time-window, whose frames can be shifted quite freely on time-axis forward or back in time (due to time-reversibility).[20]

The experimentally determined diffusion coefficient for ethanol[25] (center of mass) at 298.15 K is 1.103×10^{-5} cm^2/s, the simulation value determined by Sais et al.[26] is 1.466×10^{-5} cm^2/s, whereas the in the presented simulations we got 0.989×10^{-5} cm^2/s. The individual atom mobilities (atom-specific diffusion coefficients) are close that of the center of molecule mass ($D_{C(CH_3)} = 1.01$ cm^2/s, $D_{C(CH_2)} = 0.98$ cm^2/s, $D_{O(OH)} = 0.97$ cm^2/s). The structure predicted for liquid ethanol depends on the employed force field, the united atom approach (4 interacting points for single ethanol molecule)[23] gives different results than the all-atoms simulations presented here. The structure of liquid ethanol shows the presence of two distinctive coordination spheres (Figure 1 C), and suggests the size of the system extracted for ab initio calculations (i.e., the whole first coordination sphere with the trace of the second, $r_{OO} = 6$ Å). In Figure 1 A the analyzed subset of system is shown. In each snapshot we have from 3 to 13 ethanol molecules, and its number is statistically close to 8 (Figure 1 B).

The electronic structure calculations were done on QuantumCube cluster[27] (8 dual-dual core CPU =16 × 2.2 GHz CPU 64-bit Opteron, 16Gb RAM) using PQS software package.[27] The final calculations were obtained using 6-311++G(d,p) basis set with B3LYP potential.[28] A single step (one time frame) took from 5 to 30 min (depending on number of ethanol molecules) and the whole run (1000 time-frames) took ∼10 days. In Figure 1 D, the character of

TABLE 1: Time-Averaged Chemical Shifts for Configurations Predicted by MD Simulations, Where Isotropic Magnetic Shielding Constants Were Determined on DFT B3LYP/6-311++G(d,p)/GIAO Theory Level

	system size effect on $\langle\delta\rangle$					
	Δt = 20 ps					Δt =100ps
atom	$N_a = 1$	$N_a = 2$	$N_a = 3$	$N_a = 4$	N_a = all	$N_a = 4$
$^{\alpha}$C	54.69	53.82	54.00	54.24	54.03	54.09
$^{\beta}$C	15.01	16.45	16.25	16.02	17.26	16.92
H, (OH)	0.39	16.05	11.14	8.44	4.01	8.216
H, (CH_3)	1.54	1.43	1.51	1.48	1.47	1.46
$H^{\#}$, (CH_3)	1.36	1.33	1.37	1.42	1.46	1.50
H, (CH_3)	1.64	1.66	1.63	1.62	1.57	1.54
H (CH_2)	3.84	3.80	3.83	3.84	3.80	3.82
H, (CH_2)	4.06	3.99	4.06	4.06	3.97	4.02

TABLE 2: Time-Averaged Chemical Shifts for Configurations Predicted by MD Simulations (for All Molecules in Sphere of (N_a = *all*))[a]

		time averaged chemical shifts, Δt =					
atom	single-molecule *trans*-C_2H_5OH	10 ps	30 ps	40 ps	50 ps	100 ps	experiment
$^{\alpha}$C	66.52	54.07	54.04	53.98	53.92	**53.88**	57.0,[1,31] 58.4,[32] 57.99[33]
$^{\beta}$C	21.17	17.24	17.38	17.55	17.60	**17.63**	17.6,[1] 16.4,[32] 18.23[33]
H, (OH)	0.78	3.88	4.22	4.15	4.14	**4.30**	4.32,[1] 3.68[33]
H, (CH_3)	2.02	1.52	1.47	1.47	1.45	1.44	
$H^{\#}$, (CH_3)	1.60	1.46	1.48	1.49	1.52	1.53	
H, (CH_3)	2.02	1.55	1.56	1.54	1.52	1.51	
av	1.88	1.51	1.50	1.50	1.50	**1.49**	2.2,[1] 1.18,[30] 1.21[33]
H, (CH_2)	4.48	3.80	3.80	3.80	3.88	3.80	
H, (CH_2)	4.48	3.97	3.98	3.97	3.97	3.97	
av	4.48	3.89	3.89	3.89	3.93	**3.89**	3.59,[30] 3.38[33]

[a] The isotropic magnetic shielding constants were determined on DFT B3LYP/6-311++G(d,p)/GIAO theory level. The experimental chemical shifts and single molecule calculations are repeated from Table 4 for convenience of comparison.

variations with time of chemical shifts averaged over snapshot are shown. The Gaussian 03 package[29] was used to perform the Bader population analysis and NMR calculations with other algorithms (Supporting Information).

3. Results and Discussion

As mentioned above, the chemical shift is calculated by subtraction the isotropic magnetic shielding of a given nucleus from the reference value. For consistency, the magnetic shielding for both the molecule in question and reference molecule should be calculated at the same level of theory (Supporting Information). We include the extensive discussion of gas phase calculations in Supporting Information (comparison of ethane and ethanol, effect of rotation and bond stretching on magnetic shielding as well as charge flow characterized by Mulliken, Löwdin, Bader, and Weinhold analyses).

The effect of substitution of the $^{\alpha}$C proton is believed to generally follow the electronegativity rule of the substituent, whereas the influence on $^{\beta}$C is similar for almost for all kinds of substituents in both ^{1}H and ^{13}C NMR[1, 30]. In the vast majority of cases the substituent is more electronegative than the carbon and causes lowering of diamagnetic shielding of the carbon nucleus and the attached protons (increase in chemical shift).

According to the Mulliken, Löwdin, and Weinhold analysis the charge of the $^{\alpha}$C flows to oxygen and the $^{\beta}$C (Supporting Information). The electron densities around the methylene protons (ethanol) and the protons in ethane seem to be similar, whereas methyl protons are much poorer in electrons than methylene ones (and consequently poorer in electrons than protons in ethane). According to each analysis the oxygen atom is the strongest electron density attractor and probably the center of negative charge in the ethanol. Due to the bound oxygen, the hydroxyl proton is the poorest in electron density among other atoms (the highest positive charge). Moreover, methyl protons in the special position ($H^{\#}$) are richest in electron density among methyl protons. The analysis of chemical shift in terms of partial charges is the most straightforward estimator of electron density near given nuclei. According to the population analysis we should expect the following sequence in chemical shifts (δ) of ethanol: $^{\alpha}$C > $^{\beta}$C and H(OH) > H(CH_3) > $H^{\#}$(CH_3) > H(CH_2).

The predictions based on charge analysis are in agreement with theoretical calculations for ^{13}C NMR (molecule in gas phase) and with the experimental data (Supporting Information). However, the sequence for methyl and methylene protons is opposite in experimental and theoretical calculations, that is, even though methylene protons are richer in electron density than methyl protons they have higher chemical shift (lower magnetic shielding). Moreover, the OH proton with the highest positive charge should have the highest chemical shift, whereas it has the lowest. This suggests that population charges are not sufficient to predict the chemical shift sequence in all cases, and can be only treated as a guide. It is worth mentioning that population analysis are carried out in the absence of an external magnetic field, whereas magnetic shielding constants are obtained in its presence (as perturbation). We expect that external magnetic field could modify the charge distribution, and the population analysis on functions with perturbation corrections will produce charges in the same sequence as chemical shifts. However, the position of OH proton does not follow the population predictions, the theoretical prediction is in agreement with results of NMR spectra of gas ethanol[2]. This hypothesis will be explored in our future work.

Changes in chemical shift resulting from substitution can be also predicted using substituent constants ($\Delta\delta$), whose value is determined by fitting the experimental data.[1,30] The chemical

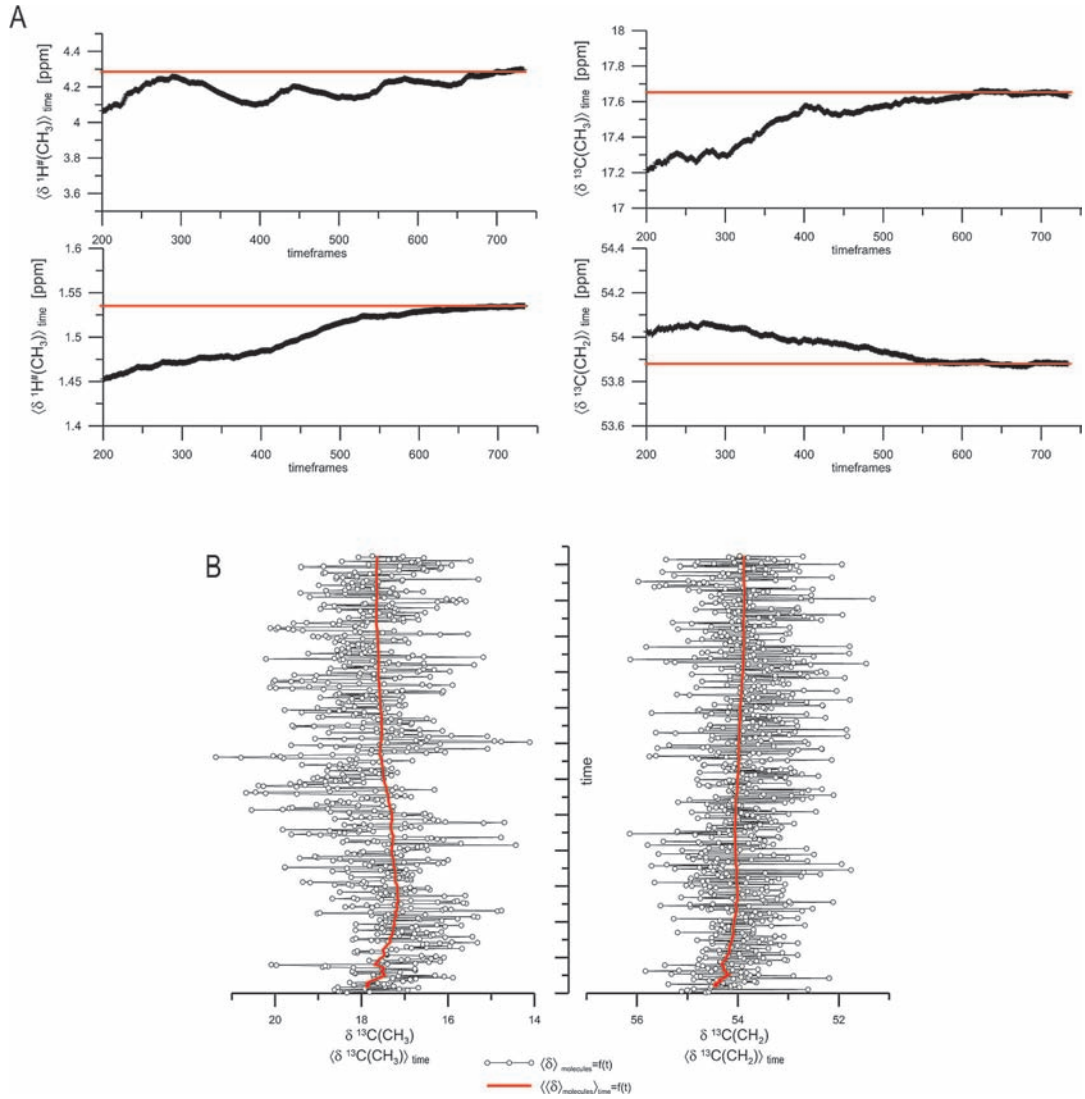

Figure 2. Relaxation of time-averaged chemical shifts (A), the red-solid line represents the hypothetical value in the thermodynamic limit (plateau on curve $\langle\delta\rangle = f(t)$). In part B, the variation of ensemble average chemical shifts and time-ensemble chemical shifts for carbon atoms are shown.

shift of $^{\alpha}$C increases about 48 ppm upon replacing H by OH, whereas the chemical shifts of the methylene protons increase about 2.56.[1,30] These rules usually work well on experimental data (Supporting Information), but they are rather rough estimations in the context of theoretical approaches, at least for GIAO NMR estimation for molecules in gas phase.

Rotation about the C−C and C−O bonds occurs with low barriers, and theoretical gas-phase predictions should be averaged over all possible conformers with an appropriate energetic weight. The energetic rotation barrier are much higher that k_BT (= 2.47 kJ/mol at T = 298 K), and the amounts of rotations are small but can occur by tunneling.

In our molecular dynamics simulations reported below, we applied constraints all molecular geometry descriptors not involved in particular motion. The difference between this simplified MM picture and unconstrained system is presented in Supporting Information. Both approaches give qualitatively similar results with the differences becoming more significant as one moves away from the *trans*-conformation. The largest disagreement is observed for *cis*-conformers, as expected reoptimized geometry has lower energy than those obtained by only rotation of *trans*-ethanol.

The empirically determined energetic rotation about the CC bond in ethane is close to 12 kJ/mol (12.6 kJ/mol,[34] 12 kJ/mol,[35] 12.3 kJ/mol[36]), whereas the theoretical estimation is: 10.9 kJ/mol,[37] 11.9 kJ/mol (10.9 with ZPVE) for internally rigid molecule and 11.3 kJ/mol (10.1 with ZPVE) for reoptimized structures (see Supporting Information). Radom, Hehre and Pople[38] estimated $\Delta\varepsilon^{rot}$ as equal to 13.6 kJ/mol (HF/4−31G). Recently, the nature and origin of rotation barrier for ethane attracted a lot of attention. Weinhold et al. claimed that hyperconjugation contributes the most to the energetic barrier estimated around 11.7 kJ/mol (MP2,CI),[39,40] whereas Mo and Gao[41] estimate barrier as 12.5 kJ/mol attributing their origin to the steric repulsion.

The rotational energetic barrier for ethanol is slightly higher than for ethane (Supporting Information). We calculate an energetic barrier for C−C torsion of 14.4 kJ/mol (13.9 with ZPVE), or 13.3 kJ/mol (12.3 with ZPVE) if we use the reoptimized geometries. Sun and Bozzelli[42] calculated this barrier theoretically to be 15.2 kJ/mol (DFT B3LYP/6-31G(d,p)).

The energetic barrier for rotation about the CO bond is 10.7 kJ/mol (9.7 with ZPVE) for the internally rigid approach and 6.1 kJ/mol (1.2 with ZPVE) for reoptimized geometries.

According to the ab initio calculations of Sun and Bozelli[42] this barrier is equal to 6.9 kJ/mol (DFT B3LYP/6-31G(d,p)), whereas Radom, Hehre, and Pople[38] estimated it as equal to

8.6 kJ/mol (HF/4−31G). In the case of rotation about CO bond, we can distinguish two energetically stable conformations: *trans* and *gauche*, with the energetic difference 5.7 kJ/mol (or 0.3 kJ/mol if we reoptimized both conformations). Jorgensen reported a *trans/gauche* energy difference of 2.1 kJ/mol (4-point force field).[23] Previous theoretical calculations give 2.7 kJ/mol,[38] ∼ 1.3 kJ/mol (DFT B3LYP/6-31G(d,p)),[42] and 1.0 kJ/mol (DFT B3LYP/6-311G(d,p)) or 0.5 kJ/mol (HF/6-311G(d,p)).[3]

The discrepancy between various theoretical estimations based on the different approach (rigid, flexible or partially flexible rotator model) as well as details of computations (basis set, approach to electron correlation, zero-point vibrations).

The difference between the chemical shifts for *trans*-ethanol and the rotationally averaged values are small, usually not exceeding 1%. In most cases rotation about CO and CC bonds decreases the chemical shifts for carbon atoms. Rotation about the CC bond generally decreases chemical shifts for hydroxyl protons, while rotation about the CO bond generally increases them (Supporting Information). The chemical shifts for methyl protons decrease if rotational motion is included, except $H^{\#}$, whose δ increases after rotational averaging. The rotation motion influences the chemical shifts of methylene protons behave similar to $H^{\#}$ (their values increase). Even if the rotational average is justified only for ideal gas molecules, for which interparticle interactions are neglected, it is generally recommended that δ be averaged over all stable conformations that are energetically possible. In the case of ethanol rotation about CO bond, the simplest estimations comprise only *gauche* and *trans* structures,[3] however the inclusion of the whole rotational spectrum seems be more correct (Supporting Information).

Because the electron density is a key factor for correct estimation of magnetic shielding constants, the electron correlations take special importance. The electron correlation is usually included by using post-Hartree−Fock methods (e.g., in our case the second-order Møller−Plesset perturbation theory) and density functional approach.

Due to the importance of precise description of electron density, the basis set size is also important. Especially, if the long-range electron correlations have to be included, diffuse functions are important. The extended discussion of effect of Hamiltonian description, basis set and other algorithms for chemical shift estimation (as implemented in Gaussian 03 package[29]) can be found in Supporting Information.

3.1. Chemical Shifts in Solvated Systems. The results of the calculations on solvated systems are shown in Tables 1 and 2. In Table 1 the effect of system size for short observation time is shown, whereas in Table 2 the effect of time-window width is presented.

The time-averaged chemical shifts for $^{\alpha}C$, methyl and methylene protons are stable even for short observation times or small system sizes (in terms number of traced molecules). This suggest that magnetic properties for these nuclei depends more on internal dynamics and interactions, which determines the structure of ethanol liquid, than on hydrogen bonding. This can be also confirmed by noticing that the short-time-averaged chemical shifts (Table 1: $\Delta t = 20$ ps, $N_a = 1$ or $\Delta t = 10$ ps, N_a = all) differ significantly from both the single-molecule calculations, and the rotationally averaged single-molecule calculations.

The time-averaged chemical shift of the OH proton is more strongly dependent on system-size than on observation-time (Table 1). Averaging the four-molecule system ($N_a = 4$) gives $\delta \sim 8$ for both $\Delta t = 20$ ps and $\Delta t = 100$ ps), whereas following all molecules in the subsystem (N_a = all) gives $\delta \sim 4$. The chemical shifts for $^{\beta}C$ seem to depend on both the system size and observation time, ($\langle\delta\rangle$) stabilizing finally around 17.6.

The behavior of time-averaged chemical shifts (Tables 1 and 2) proves that magnetic properties of $^{\beta}C$ and OH proton strongly depend on the presence of hydrogen-bonds. The $\langle\delta\rangle$ obtained by following one molecule is lower (0.39) than for single-molecule calculations (0.78), which suggest that internal dynamics and interactions in the system promotes structures where OH proton is more shielded. If more molecules are considered, the OH proton shift slowly converges with system size. The increase of observation time does not affect the average OH chemical shift.

In Figure 2A,B relaxation of the time-averaged chemical shift is shown as a function of time. In addition, in Figure 2B, the behavior of the ensemble average (over molecules in the subsystem, $\langle\delta_i\rangle_{N_a}$) and the time average ($\langle\langle\delta_i\rangle_{N_a}\rangle_{N_t}$) are shown. As pointed out previously, time-averaged chemical shifts for the $^{\alpha}C$ and the methylene and methyl protons relax much faster than for the $^{\beta}C$. Due to the formation/breaking of hydrogen-bonds the chemical shift of the OH proton shows strong fluctuations. A single molecule in the absence of solvation cannot be used to calculate the correct chemical shift for hydroxyl proton due to lack of hydrogen bonds.

The long-time behavior of the four molecule-system, which has hydrogen-bonding into the OH group, is consistent with the behavior of the larger system integrated out to shorter times, giving similar predictions for all atoms except the OH proton. This property indicates that our system is ergodic, although the hydrogen-bonding shows a dependence on cluster size.[3]

By comparing the single molecule calculations (repeated for convenience from Table 4 in the Supporting Information in Table 2) and the time-averaged values (Table 2) we see significantly better agreement with the experimental data.

The lack of internal dynamics (bond stretching, angle bending, rotation motions, interparticle interactions) inherent in ab initio calculations of NMR spectra based on single configurations do not give a reasonable results for the liquid phase. The strategy presented here seems to overcome this limitation. The theoretical results are still theory-dependent, that is, we have to choose the energy calculation scheme, basis set or functional potential as well as the algorithm for gauge-invariant magnetic shielding. The time-averaged properties define the limit of accuracy in predicting NMR spectra for liquid phase for a given level of theory.

It is important to underline some crucial aspect of presented calculations. In order to correctly treat hydrogen bonds the polarization and diffuse functions have to be included. In addition, the electron correlations are extremely important for the correct electron density profile and consequently magnetic shielding estimation, so either DFT exchange-correlation potential or one of the post-Hartree−Fock methods has to be chosen. The presented simulations still treat the ehtanol molecule as chemical entity (all covalent bonds are preserved during the simulation), a potentially more accurate approach could be pursued through ab initio molecular dynamics techniques.

4. Conclusions

The quantum cluster equilibrium approach presented by Borowski et al.[3] is able to incorporate the presence of hydrogen-bonds, however the structure of clusters does not correspond to the liquid phase, and $\delta(^1H)$ increased with cluster size to unphysical value (e.g., $\delta = 7.57$ ppm for cluster composed of 8 molecules). In our approach chemical shift for the hydroxyl proton relaxed to ∼4.3 with increases in both the system size

and in the observation time. We have shown that hydrogen-bonding substantially perturbs chemical shifts of OH proton and $^{\beta}$C, whereas the magnetic properties of other atoms depend on liquid structure (internal-dynamics, inter- and intramolecular interactions). The time-averaged chemical shifts are much closer to the experimental results than the calculation for even rotationally averaged single-molecules. Even though the actual results still depends on the theory choice for both NMR calculations as well as MD simulations, our calculations agree closely with the experimental data.

Ab-initio calculations for liquid phases are computationally demanding. In this paper we present a methodology in which the classical description (MD) is combined with the ab initio calculations. Ab initio molecular dynamics could be used to generate solvent configurations, and would probably be necessary if chemical changes were to occur in the system. However, the classical force field (OPLS/AA) has been shown to reproduce many liquid phase properties faithfully. Such properties are often incorrectly described by ab initio molecular dynamics. For this reason, in the case when the granularity of the solvent as well the special solvent/solute interactions are considered, using classical simulation methods, with an extensively tested ability to predict a correct liquid structure, may better justified.

Acknowledgment. This work was supported by Grant DE-FG02-04ER15498 from the U.S. DOE.

Supporting Information Available: Complete discussion of the calculations including tables and figures. This material is available free of charge via the Internet at http://pubs.acs.org.

References and Notes

(1) Silverstein, R. M.; Webster, F. X.,; Kiemle, D. J. *Spectrometric identification of organic compounds*; Wiley: New York, 2005.
(2) Nelson, J. H. *Nuclear Magnetic Resonance Spectroscopy*; Person Education: London, 2003.
(3) Borowski, P.; Janowski, T.; Wolinski, K. *Mol. Phys.* **2000**, *98*, 1331.
(4) Oki, M. *Application of Dynamic NMR Spectroscopy to Organic Chemistry*; VCH Publishers: Deerfield Beach, FL, 1985.
(5) Delpuech, J. J. *Dynamics of Solutions and Fluid Mixtures by NMR*, Wiley: Chichester, U.K., 1995.
(6) Karplus, M. *J. Chem. Phys.* **1959**, *30*, 11.
(7) Hinton, J. F.; Wolinski, K. Ab initio GIAO Magnetic Shielding Tensor for Hydrogen-bonded Systems. In *Theoretical Treatments of Hydrogen Bonding*; Hadzi, D., Ed.; Wiley: Chichester, U.K., 1997.
(8) Chesnut, D. B. The Ab Initio Computation of Nuclear Magnetic Resonance Chemical Shielding. In *Reviews in Computational Chemistry*; Lepkowitz, K. B., Boyd, D. B., Eds.; VCH Publishers: New York, 1996; Vol. 8.
(9) Fleischer, U.; van Wüllen, C.; Kutzelnigg, W. *NMR Chemical Shift Computation: Ab Initio in Encyclopedia of Computational Chemistry*; Wiley: New York, 1998; Vol. 3.
(10) Schindler, M.; Kutzelnigg, W. *J. Chem. Phys.* **1982**, *76*, 1919.
(11) McWenny, R. *Phys. Rev.* **1962**, *126*, 1028.
(12) Dodds, J. L.; McWenny, R.; Sadlej, A. J. *Mol. Phys.* **1980**, *41*, 1419.
(13) Wolinski, K.; Hilton, J. F.; Pulay, P. *J. Am. Chem. Soc.* **1990**, *112*, 8251.
(14) Hansen, A. E.; Stephens, P. J.; Bouman, T. D. *J. Phys. Chem.* **1991**, *95*, 4255.
(15) Keith, T. A.; Bader, R. F. W. *Chem. Phys. Lett.* **1992**, *194*, 1.
(16) Bader, R. F. W. *Atoms in Molecules, A quantum theory*; Clarendon Press; Oxford, U.K., 1994.
(17) Jensen, F. *Introduction to Computational Chemistry*; Wiley: West Sussex, U.K., 2007.
(18) Reference deleted in proof.
(19) Milner-White, E. J. *Protein Sci.* **1997**, *6*, 2477.
(20) Frenkel, D., Smith, B. *Understanding Molecular Simulation: from algorithms to applications*; Academic Press: San Diego, CA, 2002.
(21) Rapaport, D. C. *The art of molecular dynamics simulation*; Cambridge University Press: Cambridge, U.K., 2004.
(22) Jorgensen, W. *J. Am. Chem. Soc.* **1996**, *118*, 11225.
(23) Jorgensen, W. L. *J. Phys. Chem.* **1986**, *86*, 1276.
(24) Reference deleted in proof.
(25) Meckl, S.; Zeidler, M. D. *Mol. Phys.* **1988**, *63*, 85.
(26) Saiz, L.; Padró, J. A.; Guárdia, E. *J. Phys. Chem. B* **1997**, *101*, 78.
(27) Parallel Quantum Solutions. http://pqs-chem.com.
(28) Becke, A. D. *J. Chem. Phys.* **1993**, *98*, 5648.
(29) *Gaussian 03, Revision C.02*; Frisch, M. J.; Trucks, G. W.; Schlegel, H. B.; Scuseria, G. E.; Robb, M. A.; Cheeseman, J. R.; Montgomery, J. A., Jr.; Vreven, T.; Kudin, K. N.; Burant, J. C.; Millam, J. M.; Iyengar, S. S.; Tomasi, J.; Barone, V.; Mennucci, B.; Cossi, M.; Scalmani, G.; Rega, N.; Petersson, G. A.; Nakatsuji, H.; Hada, M.; Ehara, M.; Toyota, K.; Fukuda, R.; Hasegawa, J.; Ishida, M.; Nakajima, T.; Honda, Y.; Kitao, O.; Nakai, H.; Klene, M.; Li, X.; Knox, J. E.; Hratchian, H. P.; Cross, J. B.; Bakken, V.; Adamo, C.; Jaramillo, J.; Gomperts, R.; Stratmann, R. E.; Yazyev, O.; Austin, A. J.; Cammi, R.; Pomelli, C.; Ochterski, J. W.; Ayala, P. Y.; Morokuma, K.; Voth, G. A.; Salvador, P.; Dannenberg, J. J.; Zakrzewski, V. G.; Dapprich, S.; Daniels, A. D.; Strain, M. C.; Farkas, O.; Malick, D. K.; Rabuck, A. D.; Raghavachari, K.; Foresman, J. B.; Ortiz, J. V.; Cui, Q.; Baboul, A. G.; Clifford, S.; Cioslowski, J.; Stefanov, B. B.; Liu, G.; Liashenko, A.; Piskorz, P.; Komaromi, I.; Martin, R. L.; Fox, D. J.; Keith, T.; Al-Laham, M. A.; Peng, C. Y.; Nanayakkara, A.; Challacombe, M.; Gill, P. M. W.; Johnson, B.; Chen, W.; Wong, M. W.; Gonzalez, C.; and Pople, J. A.; Gaussian, Inc.: Wallingford CT, 2004.
(30) Balci, M. Basic ^{1}H−^{13}C-NMR Spectroscopy; Elsevier: Amsterdam, 2005.
(31) Lide, R. *CRC Handbook of Chemistry and Physics*; CRC Press: Boca Raton, FL, 2004.
(32) Kalinowski, H.-O.; Berger, S.; Braun, S. *Carbon-13 NMR Spectroscopy*, John Wiley & Sons: Chichester, U.K., 1988.
(33) Aldrich/ACD Library of FT NMR Spectra, 2002.
(34) Morrison, R. T.; Boyd, R. N. *Organic Chemistry*; Allan and Bacon: Boston, MA, 1966.
(35) Carey, F. C. *Organic Chemistry with Learning by Modeling*; McGraw-Hill Science; New York, 2005.
(36) Weiss, S.; Leroi, G. E. *J. Chem. Phys.* **1968**, *48*, 962.
(37) Pitzer, R. M. *Acc. Chem. Res.* **1983**, *16*, 207.
(38) Radom, L.; Hehre, W. J.; Pople, J. A. *J. Am. Chem. Soc.* **1972**, *94*, 2371.
(39) Goodman, L.; Pophristic, V.; Weinhold, F. *Acc. Chem. Res.* **1999**, *12*, 983.
(40) Weinhold, F. *Nature* **2001**, *411*, 539.
(41) Mo, Y.; Gao, J. *Acc. Chem. Res.* **2007**, *40*, 113.
(42) Sun, H.; Bozelli, J. W. *J. Phys. Chem. A.* **2001**, *105*, 9543.

JP805737A